Control of a Population of Battery Energy Storage Systems for Frequency Response

Zeyad Assi Obaid[a], L.M. Cipcigan[b], Mazin T. Muhssin[c], and Saif Sabah Sami[d]
d[a]College of Engineering, University of Diyala
Baqouba, Diyala, Iraq
d[b]Institute of Energy, School of Engineering, Cardiff University
Cardiff, Wales, United Kingdom
d[c] Faculty of Engineering, Mustansiriyah University
Baghdad, Iraq
d^d Head of Statistics Department, Mayoralty of Baghdad
Baghdad, Iraq

Abstract—The control of multiple battery energy Storage systems (BESSs) to provide frequency response will be a challenge in future smart grids. This paper proposes a hierarchical control of BESSs with two decision layers: the aggregator layer and the BESS control layer. The aggregator layer receives the states of charge (SoC) of BESSs and sends a command signal to enable/disable the BESS control layer. The BESS controller was developed to enable the BESSs to respond from the highest to lowest SoC when the frequency drops, and from lowest to highest when it rises. Hence, the BESS's response is prioritised to reduce the impact on the power system and end-users during the service. The BESS controller works independently when a failure occurs in the communication with the aggregator. The dynamic behaviour of the population of the controllable BESSs was modelled based on a Markov chain. The model demonstrates the value of aggregation of BESSs for providing frequency response and evaluates the effective capacity of the service. The model was demonstrated on the 14-machine South-East Australian power system with a 14.5GW load. 254MW of responsive capacity of aggregated batteries was effective in reducing the system frequency deviation below 0.2 Hz following a sequence of disturbances.

***Index Terms*-- Battery Energy Storage System; Demand Side Response; Frequency Regulation; Large-scale BESS aggregation; Power system Frequency Control.**

List of Abbreviations

BESS	Battery Energy Storage System
SoC	State of Charge
DLC	Direct Load Control
EVs	Electric Vehicles
DOD	Depth of Discharge
ΔF	Frequency Deviation
MSF	Membership Function
GB	Great Britain

I. Introduction

With the increased integration of renewable energy generation, system frequency control using only conventional generators becomes more expensive [1-4]. The aggregation of demand devices to regulate the frequency mitigates the need to increase the capacity of conventional power generators [1-3, 5]. In Great Britain's (GB) power system, demand side response from commercial and industrial consumers is considered for frequency control [4-8]. The term 'frequency response' in the UK refers to all dynamic and non-dynamic frequency services. Energy Storage systems are important elements of future smart grids [9-11]. BESSs have been evaluated and considered in the literature for frequency regulation [11-13].

A Markov chain has been used to represent the batteries SoC for electric vehicle (EVs) batteries [15] or PV batteries [16]. The modelling of the batteries SoC for availability of power from PV systems was presented in [16]. The model was used to improve the availability of photovoltaic generation and to represent the charge/discharge of the batteries. The dynamic representation of BESS's SoC was represented by state transitions, from zero to full charge and vice versa [16]. Various types of batteries and their applications were presented such as behind the meter BESSs (home-based) [14], smart charging of EVs [17], and large-scale BESSs (grid-scale BESS) [18]. The aggregation of these BESSs was shown to be important in regulating power system frequency [14, 17, 18].

It is anticipated that by 2025/26 in the GB power system, the fluctuation of the power from wind and solar will lead to a sharp ramp in the system demand during the day. In addition, the combination of high wind and solar output along with low demand means that a significant number of interventions by the system operator would need to be taken for system balancing and operability. Therefore, there are opportunities for demand-side services during periods of low and high demand [19].

BESSs are showing improvements in their technologies as well as cost reduction and it is estimated that storage in the GB

Z.A. Obaid is sponsored by HCED (Higher Committee for Educational Development in Iraq) to study PhD at Institute of Energy, Cardiff University, UK. (E-mail: zeyad.a.obaid@gmail.com).

power system by 2050 will be about 10.7GW based on 'Consumer Power Scenario' by the UK system operator [20]. A large number of these batteries will be in distribution systems connected behind the meter [20]. Thus, controlling a large number of distributed loads such as BESSs will be a challenge [21]. BESSs offer a fast dynamic response to compensate load variations. Controlling a large amount of distributed load such as BESSs has been investigated using centralized and decentralized control methods [22-24]. A centralized control method reduces the uncertainty in the response of controllable units. However, the centralized method has a challenge related to the communications such as the cost and latency [24]. In contrast, the decentralized control method removes this challenge, but it introduces uncertainty due to the independent response of these large distributed loads [22-24].

Many previous works have considered the control of BESSs in either centralised or decentralised control methods [12, 14, 17, 18]. However, and to the author knowledge, none of them has considered developing a control method that compromises the advantages of both centralised and decentralised control methods. Therefore, a developed control of large distributed residential and non-residential BESSs is considered in this paper to provide frequency response services in future power systems. the hierarchical control proposed in this paper is a tradeoff between the centrlised and decentrlised control methods of large distributed loads. As a result, this reduces the uncertainty associated with the response of the population during a frequency event and reduces the challenge associated with the cost and latency of the communications.

The application of BESSs in direct load control (DLC) is proposed in [14]. The combination of electrical load, its levels in the building, and their controllable devices were considered to investigate the DLC application. The problem of controlling many distributed small-scale BESSs in a building was highlighted. The scheme presented in [14] reduced the frequency deviation by controlling batteries that were installed behind the meters [14]. However, peritonising the BESSs according to their level of SoC and the value of frequency deviation was not considered in [14]. Therefore, the proposed BESSs' controller prioritises the response of the BESS based on the level of SoC. Hence, it reduces the risk of battery degradation, and the impact on the power system and the end users will be reduced.

Coordination methods were presented in [12] for controlling neighbouring batteries to regulate frequency and voltage based on local communication system on building level. However, the work presented in [12] had not consider the large problem of communication failures within a wide area power system. Therefore, The BESSs controller proposed in this paper responds, even when a failure occurs in the communication with the aggregator control layer. In addition, the speed of the BESS response is not affected by the continuously updated profile set by the central controller of the aggregator.

For the work presented in the literature, and for the author knowledge, none of them presented a control that is able to provide different frequency response services at the same time. The proposed BESS controller enables the population to participate in low and high frequency response services. In addition, the batteries' model presented previously was not presented to evaluate the effective population capacity. Therefore, the proposed model of a developed Markov chain evaluates the effective responsive capacity of the aggregated BESSs during the frequency event by considering different aggregation case studies in a multi-machine power system.

In summary, the objectives in this paper are: (i) to develop a hierarchal control of a population of BESSs; (ii) to develop a BESS controller for frequency response services; (iii) to model the population of batteries and their control to demonstrate the potential for a batteries' aggregator to offer frequency response services, and (iv) to evaluate the capacity of the aggregated batteries during the frequency event.

II. HIERARCHICAL CONTROL OF BESSS

It is assumed that BESSs with different capacities are distributed throughout the power system. A demand aggregator, which is a third-party company, aggregates these BESSs to offer frequency response services when required. This is done by integrating a controller into each BESS to control its charging/discharging processes. The demand aggregator has a central controller, which is represented by the aggregator layer (see Fig. 1). The aggregator layer collects the SoC of BESSs and sends command signals to enable/disable each BESS controller in the BESS control layer.

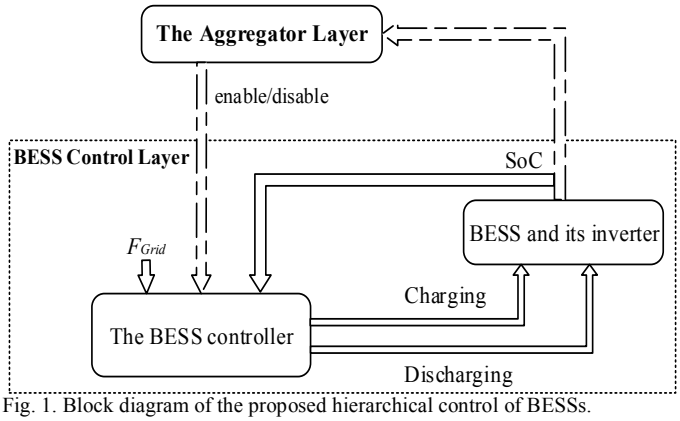

Fig. 1. Block diagram of the proposed hierarchical control of BESSs.

The battery degradation can be affected by two main factors, the number of cycles and the depth of discharge (DOD) [25]. The DOD is the level of SoC in the battery designed by the manufacturer. When the battery goes below its DOD, this will reduce the number of cycles of the battery. Therefore, the risk of reducing the life of the battery will be increased [25, 26]. Hence, considering the level of the SoC for the aggregated responsive BESSs is important as there may be hundreds of cycles each year when providing frequency response service.

Therefore, the BESS controller has pre-set frequency bands as shown in Fig. 2. The response depends on the frequency deviation and the BESS SoC. The, BESSs will respond starting from the highest level of SoC to the lowest level of SoC when the frequency drops below a nominal value. When a frequency rises above a nominal value, BESSs will respond staring from the lowest SoC to the highest SoC. As a result, the risk of a simultaneous power change of a large number of BESSs during low-frequency is reduced. In addition, prioritising the BESSs SoC reduces battery degradation.

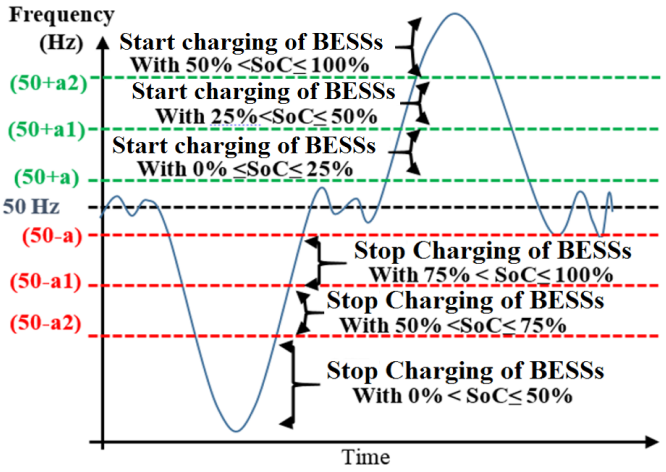

Fig. 2. The desired frequency response of the BESSs during a frequency event

Collecting the SoC values of all BESSs allows the aggregator to decide the available response capacity from the population of BESSs. In addition, in the case of discharging the BESSs and injecting power back to the grid, the proposed hierarchal control allows the aggregator to decide the response time of the BESSs according to their SoC levels. For example, the response from the BESSs with the lowest SoC can be used for the provision of primary response period (i.e. up to 10 seconds) while the BESSs with higher level of SoC can be used for longer service period such as secondary frequency response (i.e. up to 30 minutes). Therefore, the uncertainty in the response of the aggregated BESSs will be reduced during the frequency service period.

Fig. 3 displays the BESS controller, which has three main components: (i) Measurement of SoC levels, (ii) Measurements of frequency deviation and (iii) The logic gates to control the BESS charging and discharging according to (i), (ii), and the aggregator enable/disable command signal. The command signals of the aggregator control layer are either logic 1 to enable the BESS controller or logic 0 to disable it. The design of each component is explained as follows:

A. Measurements of SoC Levels

The SoC of a BESS lies within one of the following levels: 0%, 25%, 50%, 75%, and 100% SoC and Fig. 4 displays the logic outputs of the indicators of these levels which are *C1*, *C2*, *C3, C4*, and *C5*. Equations (1) - (5) were used to categorise all BESS into one of these indicators. These indicators are the input to the logic gates of BESS charging/discharging control. Considering these different levels reduces the risk of the battery degradation and the risk of a simultaneous power change at the same time.

$$C1 = \begin{cases} 1 & SoC = 0 \\ 0 & else \end{cases} \quad (1)$$

$$C2 = \begin{cases} 1 & 25\% \geq SoC > 0 \\ 0 & else \end{cases} \quad (2)$$

$$C3 = \begin{cases} 1 & 50\% \geq SoC > 25\% \\ 0 & else \end{cases} \quad (3)$$

$$C4 = \begin{cases} 1 & 75\% \geq SoC > 50\% \\ 0 & else \end{cases} \quad (4)$$

$$C5 = \begin{cases} 1 & 100\% \geq SoC > 75\% \\ 0 & else \end{cases} \quad (5)$$

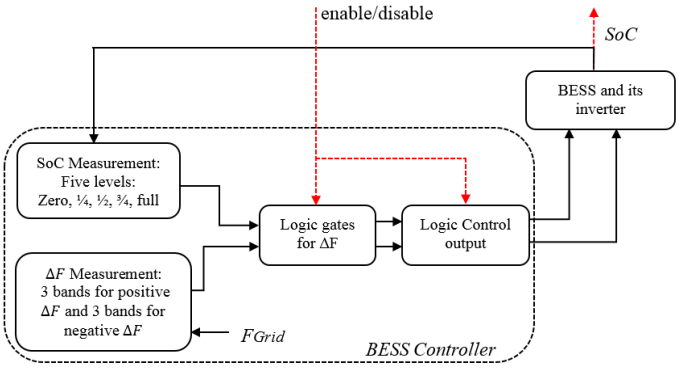

Fig. 3. Block diagram of the BESS controller.

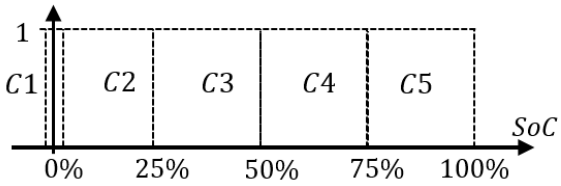

Fig. 4. Logic bands for measurements of SoC level.

B. Measurements of Frequency Deviation Levels

There are three levels of positive frequency deviations (i.e. $\Delta F_{H1,2,3}$) and three levels for negative frequency deviations (i.e. $\Delta F_{L1,2,3}$). These levels represent six bands of logic indicators as shown in Fig. 5. The system frequency deviations are located within one of these bands using equations (6) - (11), where $\Delta F = F_{Grid} - 50$. The number of these bands is set according to the aggregators' preferences and the preferred degree of the frequency response smoothness. Hence, the higher the number of bands the smoother is the response of a population of BESSs. Therefore, the proposed BESS controller enables the population to participate in both low and high frequency response services.

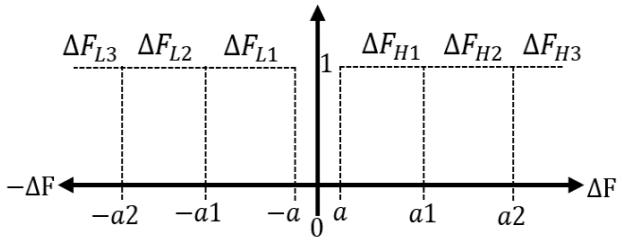

Fig. 5. Six logic frequency bands in the BESS controller.

$$\Delta F_{L1} = \begin{cases} 1 & -a \geq \Delta F \geq -a1 \\ 0 & else \end{cases} \quad (6)$$

$$\Delta F_{L2} = \begin{cases} 1 & -a1 > \Delta F \geq -a2 \\ 0 & else \end{cases} \quad (7)$$

$$\Delta F_{L3} = \begin{cases} 1 & -a2 > \Delta F \\ 0 & else \end{cases} \quad (8)$$

$$\Delta F_{H1} = \begin{cases} 1 & a1 \geq \Delta F \geq a \\ 0 & else \end{cases} \quad (9)$$

$$\Delta F_{H2} = \begin{cases} 1 & a2 \geq \Delta F > a1 \\ 0 & else \end{cases} \quad (10)$$

$$\Delta F_{H3} = \begin{cases} 1 & \Delta F > a2 \\ 0 & else \end{cases} \quad (11)$$

C. The Logic Circuits in the BESS Controller

The SoC measurements and frequency deviations measurements are used as inputs to the logic gates, the output of the logic gates and logic control output is either enable the charging /discharging of the battery when logic 1 or disable it when logic 0. The logic gates and the control output's switches are controlled by the command signal received from the aggregator control layer. Therefore, when the command signal is logic 1, the BESS will provide a frequency response by charging/discharging the BESS as shown in the logic truth table in Table I and Table II.

As a result, the BESS controller provides a response based on the last command received from the aggregator control layer. Hence, the controller works independently when any failure occurs in the communication with the aggregator control layer. Considering different levels of SoC and frequency reduces the impact on the BESS and the power system.

TABLE I
TRUTH TABLE FOR THE CONTROL OUTPUT OF THE CHARGING (NC= NO CHANGE)

Output	$C1$ 0% SoC	$C2$ 25% SoC	$C3$ 50% SoC	$C4$ 75% SoC	$C5$ 100% SoC
ΔF_{L1}	NC	NC	NC	NC	0
ΔF_{L2}	NC	NC	NC	0	0
ΔF_{L3}	0	0	0	0	0
ΔF_{H1}	1	1	NC	NC	NC
ΔF_{H2}	1	1	1	NC	NC
ΔF_{H3}	1	1	1	1	1

TABLE II
TRUTH TABLE FOR THE CONTROL OUTPUT OF THE DISCHARGING (NC= NO CHANGE)

Output	$C1$ 0% SoC	$C2$ 25% SoC	$C3$ 50% SoC	$C4$ 75% SoC	$C5$ 100% SoC
ΔF_{L1}	NC	NC	NC	NC	1
ΔF_{L2}	NC	NC	NC	1	1
ΔF_{L3}	1	1	1	1	1
ΔF_{H1}	0	0	NC	NC	NC
ΔF_{H2}	0	0	0	NC	NC
ΔF_{H3}	0	0	0	0	0

In addition, the speed of the BESS response is not affected by the continuously updated profile sent by the central controller of the aggregator. The BESS provide a fast response based on its SoC level. When the controller is enabled by logic 1 signal, it considers two factors, which are the SoC level and the value of frequency deviation. Therefore, the controller was designed with the assumption that there is no cycle limit for the controller response outside these factors.

III. MODELLING A POPULATION OF CONTROLLABLE BESSS

A model of the dynamic behaviour of BESSs was used to quantify the effective response capacity during the provision of the frequency service. This model considers the control concept of large distributed BESSs proposed in this paper. The aggregator layer collects the states of BESSs according to five different states 0%, 25%, 50%, 75%, and 100% SoC. Therefore, modelling the dynamic behaviour of the population is divided into two steps. (A) Modelling the population of BESSs at the moment just before the frequency event based on their nominal power (assumed initial condition of BESSs according to the SoC states). (B) Modelling the dynamic switching of charging/discharging operation of controllable BESSs during a frequency event, see Fig. 6.

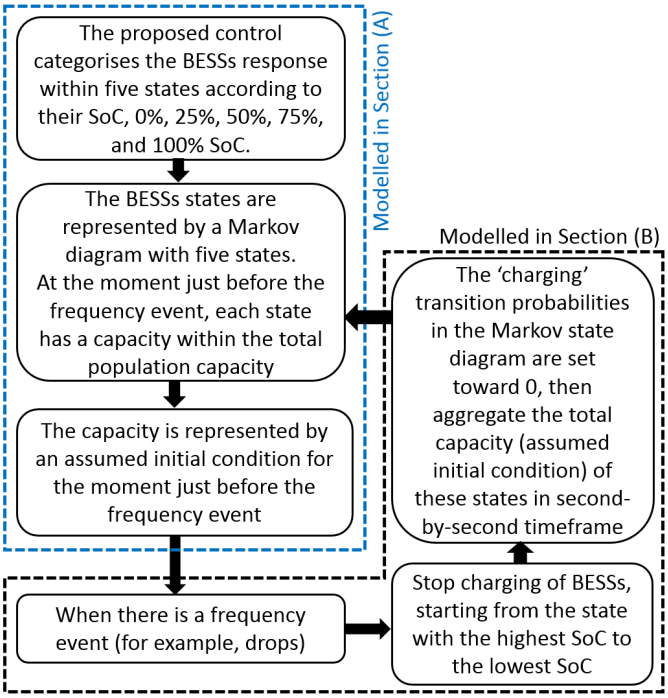

Fig. 6. Steps of modelling the dynamic behaviour of BESSs based on the proposed control scheme.

In (B), the probability of the aggregated power deviation from the population's nominal power (of (A)) during a frequency event is calculated. For example, if the population of BESSs is procured to provide the secondary frequency response service to the GB power system, its response could be sustained up to 30 minutes. Therefore, it is necessary to represent the dynamic behaviour of the aggregated power deviation of the BESS population during any service period. Markov-chain was previously used to represent dynamic behaviour of the battery SoC for electric vehicles batteries [15] or for PV charging-based batteries [15, 16]. Hence, a Markov-based model was developed to represent these two steps of the dynamic behaviour.

(A)Modelling the dynamic behaviour of the BESSs population just before a frequency event

A Markov-based state diagram was used to represent the dynamic behaviour of BESSs states as shown in Fig. 7, this Figure was drawn based on [16]. Each state represents a set of BESSs in the population according to their SoC level. The dynamic transition from the left (un-charged) to the right (fully-charged) was represented by the 'charging' transition probabilities P_1, P_2, and vice versa is by P_{-1}, P_{-2}. The probabilities of the states to remain at zero SoC and full SoC are represented by K_{11} and K_{NN}.

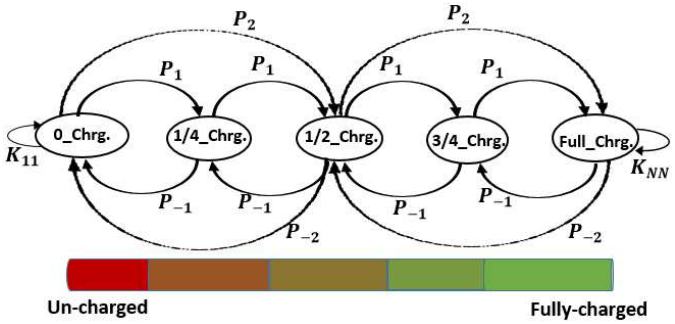

Fig. 7. State Transition Diagram is representing the dynamic behaviour of the BESSs population according to the levels of SoC (adopted from [16]).

The state diagram of Fig. 8 was represented by a 5x5 state transition matrix as presented in equation (12). Each state in Fig. 8 has an initial condition at the moment just before a frequency event. The matrix in equation (15) represents the initial conditions of the five states, where $i(1)$ represents the BESSs population with 0% SoC, and $i(5)$ represents the BESSs population with 100% SoC. This initial condition is assumed to represent the capacity of each state of BESSs at the moment just before the frequency event.

$$P(tn)=\begin{bmatrix} K_{11} & P_1 & P_2 & 0 & 0 \\ K_{11} & 0 & P_1 & P_2 & 0 \\ P_{-2} & P_{-1} & 0 & P_1 & P_2 \\ 0 & P_{-2} & P_{-1} & 0 & K_{NN} \\ 0 & 0 & P_{-2} & P_{-1} & K_{NN} \end{bmatrix}_5 \quad (12)$$

Where:

$$K_{11}=1-\sum_{i\in\{1,M\}}P_i \quad (13)$$

$$K_{NN}=1-\sum_{i\in\{1,M\}}P_{-i} \quad (14)$$

$$Pi(0)=[i(1)\ \ i(2)\ \ i(3)\ \ i(4)\ \ i(5)]_1 \quad (15)$$

(B) Modelling the dynamic switching behaviour of BESSs during a frequency event

When a frequency deviation occurs (for example, frequency drops), the population of BESSs should start responding immediately and the BESS controller prioritise the population response based on the value of ΔF and the SoC level. Therefore, the charging is stopped, starting from the BESSs with the highest to the lowest SoC.

The transition probabilities (P_1, P_2), and (P_{-1}, P_{-2}) shown in Fig. 7 have a value from 0 to 1 according to the basic concept of Markov chain [16]. Hence, to represent stop charging of the BESSs, the switching probability (P_1, P_2) will be set towards 0 and vice versa for (P_{-1}, P_{-2}). In addition, not all BESSs respond in the same time, the behaviour is a gradual transition and is dynamically linked with the level of frequency drop. The transition starts from 0 when no BESSs response and ends at 1 when all BESSs should respond.

Fuzzy membership functions (MSFs) has a gradual transition from 0 to 1[4, 27-30]. Therefore, MSFs were used to model this gradual transition behaviour of the (P_1, P_2) and (P_{-1}, P_{-2}) as shown in Fig.8.

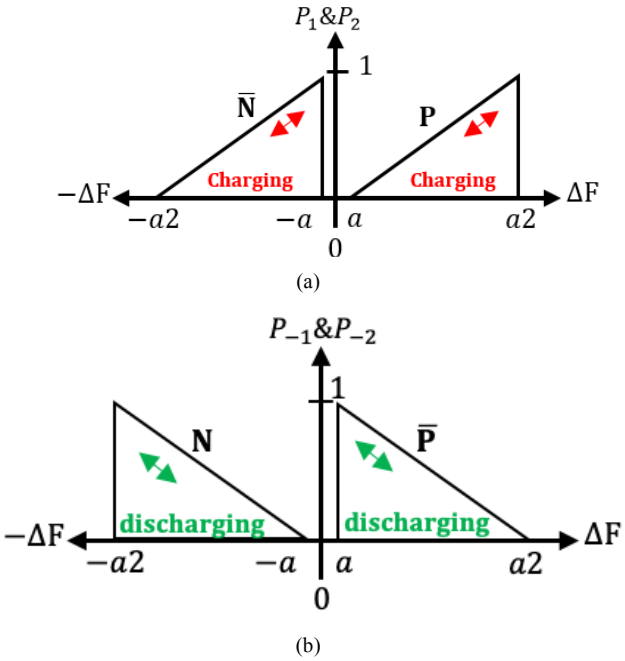

Fig. 8. The Membership Functions for the switching of the BESSs population, (a) switching probabilities into 'charging' state, (b) switching probabilities into 'discharging' state.

The population response starts with 'a' value which represents the beginning of the first frequency band and ends at 'a2' value, which represents the beginning of the last frequency band, where all BESSs should respond. The MSF dynamically updates the value of the switching probabilities (P_1, P_2) and (P_{-1}, P_{-2}) of the population. Th updated value of P_1, P_2) and (P_{-1}, P_{-2}) is according to the switching rules; P_i (for P_1, P_2) and P_{-i} (for P_{-1}, P_{-2}) as shown in equations (16) and (17).

$$P(_i)=\begin{cases} P & if\ \Delta F \geq a \\ \overline{N} & if\ \Delta F \leq -a \end{cases} \quad (16)$$

$$P(_{-i})=\begin{cases} \overline{P} & if\ \Delta F \geq a \\ N & if\ \Delta F \leq -a \end{cases} \quad (17)$$

The updated values of (P_1, P_2) and (P_{-1}, P_{-2}) are used to dynamically re-update the state transition matrix of equation (12). Therefore, the initial condition of the five states, which represented the capacity of the BESSs states before the frequency deviation, are then dynamically updated during the frequency drop/rise period. This is done in a second-by-second timeframe using equation (18). Where, $P(tn)$ is the new state transition matrix with the updated values of (P_1, P_2) and (P_{-1}, P_{-2}).

$$P(tn+1)_1=Pi(0)\ P(tn) \quad (18)$$

The dynamic aggregation of the total responsive capacity of the population of BESSs is done by using Equation (19). Combining equations (19) and (20) results in equation (21), where $P(1)$ to $P(5)$ represent the dynamic updated initial condition (capacity) of each state after a frequency drop/rise.

$$Yi(tn) = [P(tn+1)]\, C \tag{19}$$

$$C = \begin{bmatrix} C1 \\ C2 \\ C3 \\ C4 \\ C5 \end{bmatrix}_{5*1} \tag{20}$$

$$Yi(tn) = [C1xP(1) + C2xP(2) + C3xP(3) + C4xP(4) + C5xP(5)] \tag{21}$$

The dynamic aggregation is implemented based on the proposed control scheme using matrix '*C*'. This is done by assigning the value of the matrix's parameters (*C1*, *C2* ….) to either 0 or 1 according to the value of ΔF as explained in section II. For example, to stop charging of BESSs with 75% SoC and 100% SoC during the second frequency band, (between '*a1*' and '*a2*'), parameters *C1*, *C2*, and *C3* are set to 0, while *C4* and *C5* are set to 1. The power deviation of the BESSs population is calculated using equation (22), where the responsive capacity of the BESSs in (21) is subtracted from the total capacity of the aggregated BESSs ($Ptot$).

$$Y(tn)_1 = Ptot - Yi(tn) \tag{22}$$

For example, when ΔF= -0.08 Hz where ΔF = FGrid -50, at this moment, the grid frequency is less than the nominal frequency and the controlled demand must be responded. The $P(_i)$= $\overline{\overline{N}}$ and $P(_{-i})$= N according to the Fig. 9 and the response is under the control of N *and* $\overline{\overline{N}}$. The control is also linked with the battery SoC according to Fig.4, the controlled demand will be responded for all batteries above 50% SoC. Equations 18 and 19 will dynamically updated to calculate the total responded capacity.

The flowchart shown in Fig.9 represents the complete modelling of the proposed control of BESSs for the negative ΔF bands (when the frequency drops). When the frequency goes below a nominal value '-a1', the prosed dynamic model of BESSs population is activated. The proposed control which associated with the dynamic model selects the response of controllable batteries according to the proposed criterion, which is based on the value of ΔF and the level of SoC. Finally, the dynamic aggregation will be updated to calculated the responded capacity. The complete flowchart for the positive ΔF is the same as in Fig. 9, except the value of ΔF for the value of a, a1, and a2 will be for the right side of Fig. 5.

IV. Demonstration of The Proposed Control of BESSs.

The modelling and simulation results of the controllable BESSs are carried out using MATLAB® and MATLAB®/SimPowerSystems™. Comparing to previous work which was done on a small representation of power system, the 14-machines South-East Australian power system was used to evaluate the proposed control scheme (see Fig. 10). This large dynamic benchmark power system with load case 4 [31, 32] was used as the base case of the system load, which is approximately 14.5GW. this an opportunity to increase the realistic of the response behaviour than work presented in the literature. This system contains a primary droop-based frequency response. No other frequency control loop is considered in this work.

The results are stored as vectors to visualise and compare the results. This model was used for testing new control techniques in a power system; further details were presented in [31, 32]. The control of a population of BESSs was implemented using a dynamic controllable load. Each controllable load represents an Aggregator for different size of BESSs. Three different Aggregators in different areas are considered as shown in Table III and Fig. 10.

The proposed control is applicable for any battery size in a resedintional or non-residentional uses. Therefore, the requirement of the battery size was left to the aggregator and the market preferences and was not covered in this paper.

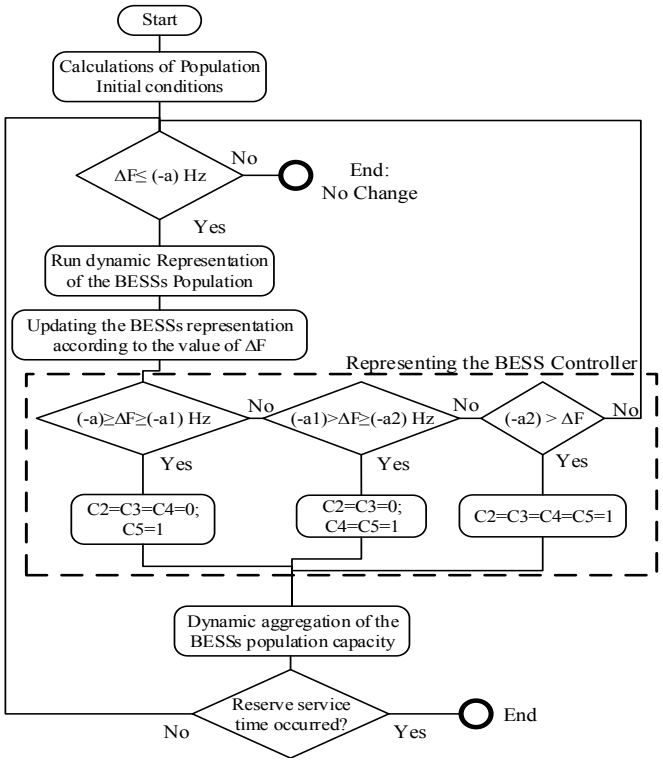

Fig. 9. Flow chart of the modelling of the proposed control of BESSs.

TABLE III
AGGREGATORS AND THEIR BESSS POPULATION ASSUMPTION TYPES

	Non-Residential BESSs (MW)	Residential BESSs (MW)	Total (MW)
1-Bus 206 (area 2)	30	50	80
2-Bus 312 (area 3)	42	50	92
3-Bus 408 (area 4)	50	60	110

A large frequency disturbance was considered which recently took place on 28th of September 2016 in the South Australian power system to evaluate the proposed population control. The disturbance started when 123MW of wind generation were lost followed by another loss of 192MW wind generation after 6

seconds. This loss of approximately 311MW generation led to 560MW interconnector tripping. This event of generation and interconnectors loss sequence was modelled and applied to the test system at t=5s, t=11s, and t=13s, and the simulation results were captured. This disturbance was simulated as a sudden increase in the load at busbar 405 near generator GPS_4 in area 4 (see Fig. 10), the impact of the location of the disturbance was out of the scope of this paper.

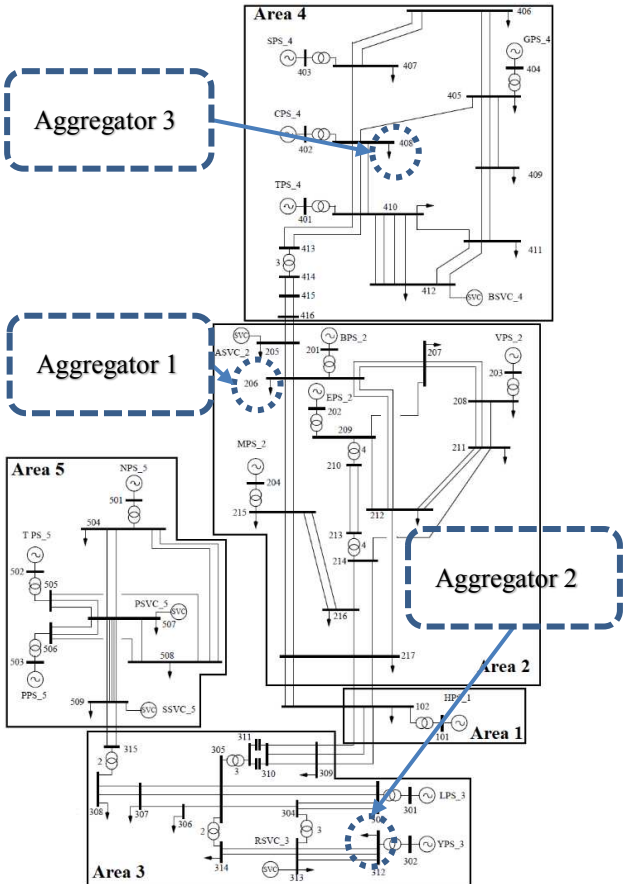

Fig. 10. IEEE 14-generator 59-bus, 5-areas, The South East Australian Power System [32, 33].

Three case studies are considered to represent three realistic possibilities to integrate different aggregators with different capacities (see Table IV). Also, the initial condition of BESSs according to the level of SoC is assumed as shown in Table V. In addition, the frequency bands parameters, *a*, *a1*, and *a2* also have an impact on the population response. Therefore, three different values were considered for the simulation comparison as shown in Table VI.

TABLE IV
STUDY CASES FOR THE SIMULATION RESULTS WITH THE SOUTH EAST AUSTRALIAN POWER SYSTEM

	Study cases		
aggregator at:	A1 (MW)	A2 (MW)	A3 (MW)
1-Bus 206 (area 2)	80	80	80
2-Bus 312 (area 3)	0	0	110
3-Bus 408 (area 4)	0	92	92
Total (MW)	**80**	**172**	**282**

TABLE V
SOC INITIAL CONDITIONS STUDY CASES

	0% SoC (*C1*)	25% SoC (*C2*)	50% SoC (*C3*)	75% SoC (*C4*)	100% SoC (*C5*)
Pi(0)	0.1	0.1	0.1	0.3	0.4

TABLE VI
DIFFERENT VALUES OF FREQUENCY BANDS PARAMETERS

	a	*a1*	*a2*
Value 1 (Hz)	0.015	0.05	0.1
Value 2 (Hz)	0.015	0.03	0.05
Value 3 (Hz)	0.015	0.02	0.04

Scenario 1: Different cases of the aggregation capacity

In this section, the aggregators' cases shown in Table IV and value 1 in Table VI are considered. Increasing the number of aggregators and the amount of controllable BESSs leads to a significant reduction in the frequency deviation and frequency error (see Fig. 11). In case of A3, there are three aggregators with 282MW of controllable BESSs and initial SoC levels as shown in Table V, which reduces the highest frequency deviation from 0.23 Hz to 0.15 Hz for the biggest disturbance sequence at *t=13s*.

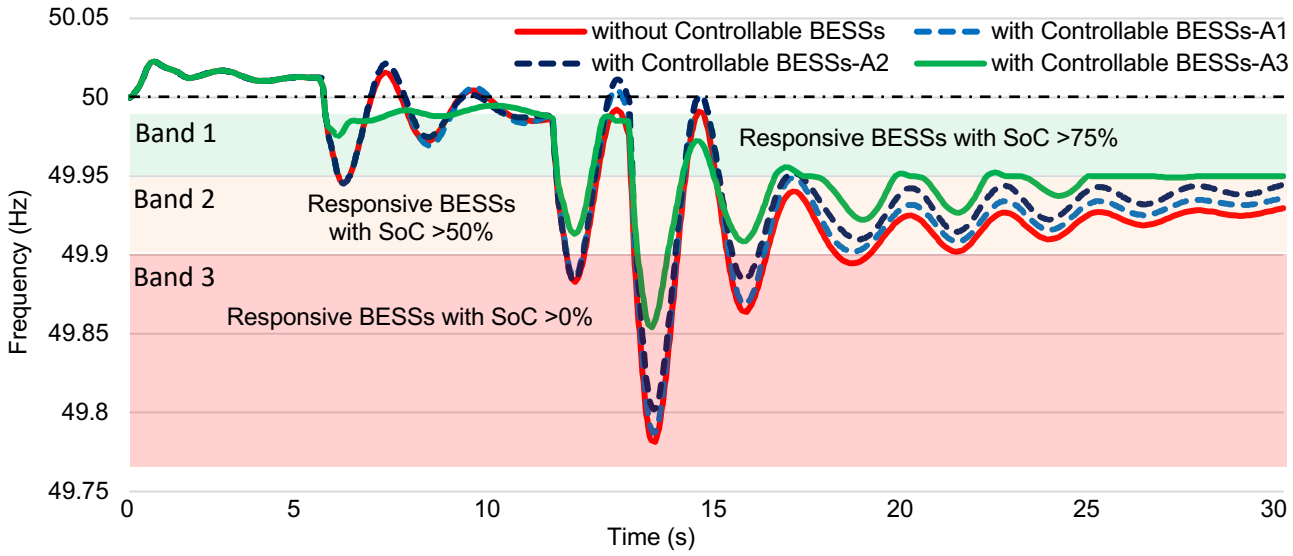

Fig. 11. Frequency response at Power Station of busbar 404 in *Scenario 1* with the aggregators' cases in Table IV.

Other bands comparison is shown in Table VII with the responsive capacity of each aggregation case study. Case A1 and Case A2 provided less impact on the response, which is reasonable due to their capacity against the size of the disturbance.

TABLE VII
COMPARISON OF THE RESULTS SHOWN IN FIG. 12 USING SOC INITIALS OF TABLE V ACCORDING TO THE CONTROL SCHEME PROPOSED IN FIG. 2

at	Frequency limit	Total responsive capacity of BESSs		Max value of ΔF (Hz)
Band 1 (Green)	Below 49.985 (ΔF ≤ -0.015)	A1	0.4*80= 32 MW	0.06
		A2	0.4*172= 68.8 MW	0.06
		A3	0.4*282= 112.8 MW	0.03
Band 2 (Orang)	Below 49.95 (ΔF ≤ -0.05)	A1	0.7*80= 56 MW	0.12
		A2	0.7*172= 120.4 MW	0.12
		A3	0.7*282= 197.4 MW	0.09
Band 3 (Red)	Below 49.9 (ΔF ≤ -0.1)	A1	0.9*80= 72 MW	0.22
		A2	0.9*172= 154.8 MW	0.20
		A3	0.9*282= 253.8 MW	0.15

Scenario 2: Different value of frequency bands

In this section, different values of '*a*, *a1*, *a2*' (Table VI) and case A3 in Table IV were considered, these values are set by an aggregator and can be updated if necessary. Through these values, the BESS response can be controlled according to frequency bands and SoC levels. These values have an impact on the frequency response of the population of BESSs. The reduction of the values of the bands improved the frequency response and vice versa (see Fig. 12). The impact of the reduction is in relation to the aggregation capacity and the service type (i.e. frequency regulation, primary or secondary... etc.).

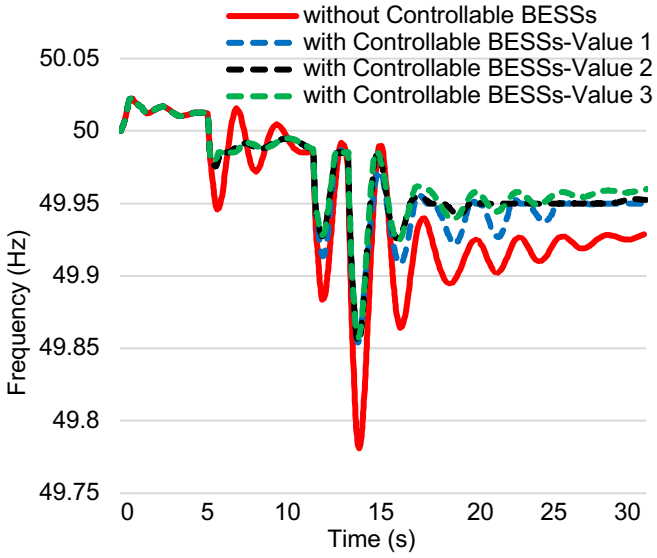

Fig. 12. Frequency response at power station of busbar 404 in Scenario 2 using different values of frequency bands in Table VI.

There was an oscillatory behaviour in the response in Fig. 11 and Fig. 12. The largest responsive capacity was about 250MW in A3 simulation cases, while the total disturbance was more than 800MW. Therefore, this oscillatory in this situation is a normal behaviour due to this huge disturbance comparing to real cases occurred in the litrature. The simulation results in this paper proposed more realistice frequency response behaviour than work presented in the litarture such the work presented in [12, 14, 17, 18, 12, 24].

V. CONCLUSIONS

A hierarchical control was proposed to aggregate different size of BESSs to provide frequency response services. The BESS controller can respond to either negative or positive frequency deviations. Hence, can participate in either high or low-frequency response services. The BESS controller also enables BESS to work independently when any failure occurs in the communications with the aggregator.

A model of a population of BESSs was developed for the proposed hierarchical control to demonstrate the potential to provide frequency response service and to evaluate the effective capacity during a frequency event. The model divides the population of BESSs into five states based on their SoC, and dynamically control the BESSs according to their SoC levels during the provision of frequency response services.

The control scheme was demonstrated using various case studies on the 14-machines South-East Australian power system. Comparing to previous work, a large dynamic benchmark system with a system load base equal to 14.5GW was used in this work to demonstrate the proposed design. A 253.8MW of responsive capacity of controllable BESSs was effective in reducing frequency deviations following a large simulated real disturbance sequence.

Considering the battery SoC to reduce the risk of battery degradation and not to affect the user comfort, and eliminating the cost of real-time communications, enables the proposed control of BESSs to be applied in (i) Residential and non-residential BESSs, (ii) Large-scale BESSs, and (iii) Vehicle-to-Grid (V2G), and (iv) Virtual Power Plant (VPP). In addition, the proposed design is applicable to provide high frequency response services, hence, it is recommended for future work to demonstrate the effective responsive capacity for this service.

REFERENCES

[1] K. K. Marcelo A. Elizondo, Christian Moya Calderon and Wei Zhang, "Frequency Responsive Demand in U.S. Western Power System Model," in IEEE Power & Energy Society General Meeting, 26-30 July 2015, pp. 1 - 5.

[2] J. H. K Kalsi, J Fuller, LD Marinovici, M Elizondo, T Williams, J Lian, Y Sun, *Loads as a Resource Frequency Responsive Demand*, Prepared for the U.S. Department of Energy under Contract DE-AC05-76RL01830, Pacific Northwest National Laboratory Richland, Washington 99352, December 2015.

[3] J. L. K Kalsi, LD Marinovici, M Elizondo, W Zhang and C Moya, *Loads as a Resource Frequency Responsive Demand*, Prepared for the U.S. Department of Energy under Contract DE-AC05-76RL01830, Pacific Northwest National Laboratory Richland, Washington 99352, September 2014.

[4] M. T. Muhssin, L. M. Cipcigan, N. Jenkins, C. Meng, and Z. A. Obaid, "Modelling of a population of Heat Pumps as a Source of load in the Great Britain power system," in 2016 International Conference on Smart Systems and Technologies (SST), 2016, pp. 109-113.

[5] Z. A. Obaid, L. M. Cipcigan, and M. T. Muhssin, "Design of a Hybrid Fuzzy/Markov Chain-based Hierarchal Demand-side Frequency Control," in IEEE PES GM, 2017, Chicago. USA, 2017, pp. 1-5.

[6] V. Trovato, F. Teng, and G. Strbac, "Value of thermostatic loads in future low-carbon Great Britain system." pp. 1-7.

[7] V. Trovato, S. H. Tindemans, and G. Strbac, "Demand response contribution to effective inertia for system security in the GB 2020

gone green scenario." IEEE PES ISGT Europe, pp. 1-5, 6-9 Oct. 2013.

[8] V. Trovato, I. M. Sanz, B. Chaudhuri, and G. Strbac, "Advanced Control of Thermostatic Loads for Rapid Frequency Response in Great Britain," *IEEE Transactions on Power Systems,* vol. PP, no. 99, pp. 1-1, 2016.

[9] M. Cheng, S. S. Sami, and J. Wu, "Benefits of using virtual energy storage system for power system frequency response," *Applied Energy*, 2016.

[10] J. Li, R. Xiong, Q. Yang, F. Liang, M. Zhang, and W. Yuan, "Design/test of a hybrid energy storage system for primary frequency control using a dynamic droop method in an isolated microgrid power system," *Applied Energy*, 2016.

[11] Z. A. Obaid, L. Cipcigan, and M. T. Muhsin, "Analysis of the Great Britain's power system with Electric Vehicles and Storage Systems," in 2015 18th International Conference on Intelligent System Application to Power Systems (ISAP), 2015, pp. 1-6.

[12] S. J. Lee, J. H. Kim, C. H. Kim, S. K. Kim, E. S. Kim, D. U. Kim, K. K. Mehmood, and S. U. Khan, "Coordinated Control Algorithm for Distributed Battery Energy Storage Systems for Mitigating Voltage and Frequency Deviations," *IEEE Transactions on Smart Grid,* vol. 7, no. 3, pp. 1713-1722, May, 2016.

[13] S. S. Sami, C. Meng, and W. Jianzhong, "Modelling and control of multi-type grid-scale energy storage for power system frequency response." IEEE 8th International Power Electronics and Motion Control Conference (IPEMC-ECCE Asia), pp. 269-273, 22-26 May 2016.

[14] Y.-J. Kim, G. Del-Rosario-Calaf, and L. K. Norford, "Analysis and Experimental Implementation of Grid Frequency Regulation Using Behind-the-Meter Batteries Compensating for Fast Load Demand Variations," *IEEE Transactions on Power Systems,* vol. 32, no. 1, pp. 484-498, 2017.

[15] E. B. Iversen, J. M. Morales, and H. Madsen, "Optimal charging of an electric vehicle using a Markov decision process," *Applied Energy,* vol. 123, pp. 1-12, Jun 15, 2014.

[16] J. Song, V. Krishnamurthy, A. Kwasinski, and R. Sharma, "Development of a Markov-Chain-Based Energy Storage Model for Power Supply Availability Assessment of Photovoltaic Generation Plants," *IEEE Transactions on Sustainable Energy,* vol. 4, no. 2, pp. 491-500, Apr, 2013.

[17] Y. Tang, J. Zhong, and M. Bollen, "Aggregated optimal charging and vehicle-to-grid control for electric vehicles under large electric vehicle population," *IET Generation, Transmission & Distribution,* vol. 10, no. 8, pp. 2012-2018, 2016.

[18] S. M. Alhejaj, and F. M. Gonzalez-Longatt, "Impact of inertia emulation control of grid-scale BESS on power system frequency response." International Conference for Students on Applied Engineering (ICSAE), pp. 254-258, 20-21 Oct. 2016.

[19] N. Grid, *System Operability Framework 2016*, National Grid, 2016.

[20] N. Grid, *Future Energy Scenario*, 2017.

[21] A. C. Chapman, and G. Verbic, "Dynamic distributed energy resource allocation for load-side emergency reserve provision." 2016 IEEE Innovative Smart Grid Technologies - Asia (ISGT-Asia), pp. 1189-1194, Nov. 28 2016-Dec. 1 2016.

[22] N. Lu, "An evaluation of the HVAC load potential for providing load balancing service," *IEEE Transactions on Smart Grid,* vol. 3, no. 3, pp. 1263-1270, 2012.

[23] J. A. Short, D. G. Infield, and L. L. Freris, "Stabilization of Grid Frequency Through Dynamic Demand Control," *IEEE Transactions on Power Systems,* vol. 22, no. 3, pp. 1284-1293, 2007.

[24] S. S. Sami, "Virtual Energy Storage for Frequency and Voltage Control," Institute of Energy, Cardiff University, 2017.

[25] B. Xu, A. Oudalov, A. Ulbig, G. Andersson, and D. S. Kirschen, "Modeling of Lithium-Ion Battery Degradation for Cell Life Assessment," *IEEE Transactions on Smart Grid,* vol. 9, no. 2, pp. 1131-1140, 2018.

[26] B. Lian, A. Sims, D. Yu, C. Wang, and R. W. Dunn, "Optimizing LiFePO4 Battery Energy Storage Systems for Frequency Response in the UK System," *IEEE Transactions on Sustainable Energy,* vol. 8, no. 1, pp. 385-394, 2017.

[27] L. M. C. Mazin T Muhssin, Zeyad A Obaid and Wissam F AL-Ansari, "A novel adaptive deadbeat- based control for load frequency control of low inertia system in interconnected zones north and south of Scotland," *International Journal of Electrical Power & Energy Systems,* vol. 89, pp. 52-61, 2017.

[28] M. T. Muhssin, L. M. Cipcigan, and Z. A. Obaid, "Small Microgrid stability and performance analysis in isolated island," in 2015 50th International Universities Power Engineering Conference (UPEC), 2015, pp. 1-6.

[29] Z. A. Obaid, N. Sulaiman, and M. N. Hamidon, "Design of fuzzy logic controller for AC motor based on field programmable gate array." 2009 IEEE Student Conference on Research and Development (SCOReD), pp. 487-490, Malaysia, 16-18 Nov. 2009.

[30] Z. A. Obaid, L. M. Cipcigan, and M. T. Muhssin, "Fuzzy hierarchal approach-based optimal frequency control in the Great Britain power system," *Electric Power Systems Research,* vol. 141, pp. 529-537, Dec, 2016.

[31] A. Moeini, I. Kamwa, P. Brunelle, and G. Sybille, "Open data IEEE test systems implemented in SimPowerSystems for education and research in power grid dynamics and control." in 50th International Universities Power Engineering Conference (UPEC), UK, pp. 1-6, 1-4 Sept. 2015.

[32] R. R. a. I. Hiskens, *IEEE PES Task Force on Benchmark Systems for Stability Controls-Technical Report*, IEEE, 2015.

[33] M. G. a. D. Vowles, *Simplified 14-Generator Model of the South East Australian Power System*, School of Electrical & Electronic Engineering, The University of Adelaide, South Australia, 2014.